The Measurement of AM noise of Oscillators

Enrico Rubiola
FEMTO-ST Institute
UMR 6174, CNRS and Université de Franche Comté
32 av. de l'Observatoire, Besançon, France

home page: http://rubiola.org
e-mail: rubiola@femto-st.fr

***Abstract*— The close-in AM noise is often neglected, under the assumption that it is a minor problem as compared to phase noise. With the progress of technology and of experimental science, this assumption is no longer true. Yet, information in the literature is scarce or absent.**

This article describes the measurement of the AM noise of rf/microwave sources in terms of $S_\alpha(f)$, i.e., the power spectrum density of the fractional amplitude fluctuation α. The proposed schemes make use of commercial power detectors based on Schottky and tunnel diodes, in single-channel and correlation configuration. There follow the analysis of the methods for the measurement of the power-detector noise, and a digression about the calibration procedures. The measurement methods are extended to the relative intensity noise (RIN) of optical beams, and to the AM noise of the rf/microwave modulation in photonic systems.

Some rf/microwave synthesizers and oscillators have been measured, using correlation and moderate averaging. As an example, the flicker noise of a low-noise quartz oscillator $S_\alpha = 1.5\times10^{-13}/f$, which is equivalent to an Allan deviation of $\sigma_\alpha = 4.6\times10^{-7}$. The measurement systems described exhibit the world-record lowest background noise.

An extended version of this article is available on the arXiv web site, document axXiv:physics/0512082.

I. Basics

A quasi-perfect—that is, low-noise—rf/microwave sinusoidal signal can be written as

$$v(t) = V_0\big[1+\alpha(t)\big]\cos\big[2\pi\nu_0 t + \varphi(t)\big] \quad , \tag{1}$$

where $\alpha(t)$ is the fractional amplitude fluctuation, and $\varphi(t)$ is the phase fluctuation. Equation (1) defines $\alpha(t)$ and $\varphi(t)$.

It is often convenient to describe the close-in noise in terms of the single-side power spectral density $S(f)$, as a function of the Fourier frequency f. A model that has been found useful to describe $S(f)$ is the power-law $S(f) = \sum_i h_i f^i$. In the case of amplitiude noise, generally the spectrum contains only the white noise $h_0 f^0$, the flicker noise $h_{-1}f^{-1}$, and the random walk $h_{-2}f^{-2}$. Accordingly,

$$S_\alpha(f) = h_0 + h_{-1}f^{-1} + h_{-2}f^{-2} \quad . \tag{2}$$

Random walk and higher-slope phenomena, like drift, are often induced by the environment. It is up to the experimentalist to judge the effect of environment.

The spectrum density can be converted into Allan variance using the formulae of Table I, which are the formulae commonly used for the frequency-fluctuation spectrum $S_y(f)$.

TABLE I
Power spectrum density and Allan variance.

noise type	Spectrum density $S_\alpha(f)$	Allan variance $\sigma^2_\alpha(\tau)$
white	h_0	$\dfrac{h_0}{2\tau}$
flicker	$h_{-1}f^{-1}$	$h_{-1}\ 2\ln(2)$
random walk	$h_{-2}f^{-2}$	$h_{-2}\ \dfrac{4\pi^2}{6}\,\tau$

The signal power is

$$P = \frac{V_0^2}{2R}\big(1+\alpha\big)^2 \tag{3}$$

thus

$$P \simeq \frac{V_0^2}{2R}\big(1+2\alpha\big) \qquad \text{because } \alpha \ll 1 \tag{4}$$

It is convenient to rewrite P as $P = P_0 + \delta P$, with

$$P_0 = \frac{V_0^2}{2R} \qquad \text{and} \qquad \delta P \simeq 2P_0\alpha \tag{5}$$

The amplitude fluctuations are measured through the measurement of the power fluctuation δP,

$$\alpha(t) = \frac{1}{2}\frac{\delta P}{P_0} \tag{6}$$

and of its power spectrum density,

$$S_\alpha(f) = \frac{1}{4}S_{\frac{P}{P_0}}(f) = \frac{1}{4P_0^2}S_P(f) \ . \tag{7}$$

This article focus on the measurement of oscillators and other sources, where bridge techniques can not be exploited. Conversely, the measurement of two-port devices, like the amplifier, is made easy by the availability of the reference signal sent to the device input. In this case, the bridge (interferometric) method [1] enables the measurement of amplitude noise and phase noise with outstanding sensitivity.

II. Experimental method

A. Single channel measurement

Figure 1 shows the basic scheme for the measurement of AM noise. Looking at one channel, the detector characteristics (Sec. III) is $v_d = k_d P$, hence the ac component of the detected

1-4244-0074-0/06/$20.00 © 2006 IEEE.

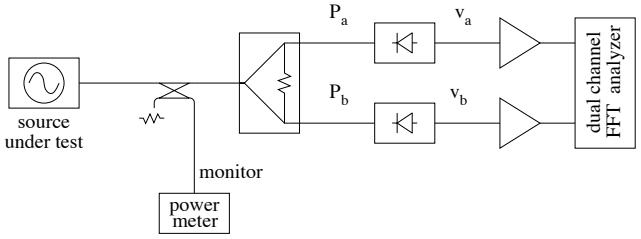

Fig. 1. Correlation AM noise measurement.

signal is $\tilde{v}_d = k_d \delta P$. The subscript '$d$' is either a or b. The detected voltage is related to α by $\tilde{v}_d = k_d P_0 \frac{\delta P}{P_0}$, that is,

$$\tilde{v}_d(t) = 2k_d P_0 \alpha(t) \quad . \tag{8}$$

Turning voltages into spectra, the above becomes

$$S_v(f) = 4k_d^2 P_0^2 S_\alpha(f) \quad . \tag{9}$$

Therefore, the spectrum of α can be measured using

$$S_\alpha(f) = \frac{1}{4k_d^2 P_0^2} S_v(f) \quad . \tag{10}$$

Due to linearity of the network that precedes the detector (directional couplers, cables, etc.), the fractional power fluctuation $\delta P/P_0$ is the same in all the circuit, thus α is the same. As a consequence, the separate measurement of the oscillator power and of the attenuation from the oscillator to the detector is not necessary. The straightforward way to use Eq. (9), or (10), is to refer P_0 at detector input, and v_d at the detector output.

Interestingly, phase noise has virtually no effect on the measurement. This happens because the bandwidth of the detector is much larger than the maximum frequency of the Fourier analysis, hence no memory effect takes place.

In single-channel measurements, the background noise can only be assessed by measuring a trusted low-noise source, which can not be validated. For this reason, the dual-channel scheme is used whenever possible.

B. Dual channel (correlation) measurement

The signal is split into two branches, and measured by two separate power detectors and amplifiers (Fig. 1). Under the assumption that the two channels are independent, the cross spectrum $S_{ba}(f)$ is proportional to $S_\alpha(f)$. In fact, the two dc signals are $v_a = k_a P_a \alpha$ and $v_b = k_b P_b \alpha$. The cross spectrum is

$$S_{ba}(f) = 4k_a k_b P_a P_b S_\alpha(f) \quad , \tag{11}$$

from which

$$S_\alpha(f) = \frac{1}{4k_a k_b P_a P_b} S_{ba}(f) \quad . \tag{12}$$

Averaging over m spectra, the noise of the individual channels is rejected by a factor $\sqrt{2m}$, for the sensitivity can be significantly increased. A further advantage of the correlation method is that the measurement of $S_\alpha(f)$ is validated by the simultaneous measurement of the instrument noise limit, that is, the single-channel noise divided by $\sqrt{2m}$.

Gain is proportional to power (Eq. (11)). In a correlation system, the total power P_0 is split into the two channels, for $P_a P_b = \frac{1}{4} P_0^2$. Hence, switching from single-channel to correlation the gain drops by a factor $\frac{1}{4}$ (-6 dB), for larger m is necessary. Yet, in a number of practical cases this does not happen because the available power is larger than twice the detector maximum input power.

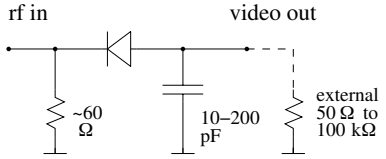

Fig. 2. Scheme of the diode power detector.

TABLE II
SOME POWER-DETECTOR MANUFACTURERS.

manufacturer	web site
Aeroflex/Metelics	aeroflex-metelics.com
Agilent Technologies	agilent.com
Advanced Control Components	advanced-control.com
Advanced Microwave	advancedmicrowaveinc.com
Eclipse	eclipsemicrowave.com
Herotek	herotek.com
Microphase	microphase.com/military/detectors.shtml
Omniyig	omniyig.com
RLC Electronics	rlcelectronics.com/detectors.htm
S-Team	s-team.sk

III. SCHOTTKY AND TUNNEL DIODE POWER DETECTORS

A rf/microwave power detector uses the nonlinear response of a diode to turn the input power P into a dc voltage v_d. The transfer function is

$$v_d = k_d P \quad , \tag{13}$$

which defines the detector gain k_d. The physical dimension of k_d is A^{-1}. The technical unit often used is mV/mW, equivalent to A^{-1}. The diode work as a power detector at low input level, and turns smoothly into an envelope detector beyond a threshold power.

Figure 2 shows the scheme of actual power detectors. The input resistor matches the high input impedance of the diode network to the standard value $R_0 = 50\ \Omega$ over the bandwidth and over the power range. The value depends on the specific detector. The output capacitor filters the video signal, eliminating the carrier from the output. A low capacitance makes the detector fast, while a higher capacitance may be needed to demodulate a low-frequency carrier.

Power detectors are available off-the-shelf from numerous manufacturers, some of which are listed on Table II. Agilent Technologies provides a series of useful application notes [2] about the measurement of rf/microwave power. Two types of diode are used in practice, Schottky and tunnel. Their typical characteristics are shown in Table III.

Schottky detectors are the most common ones. The relatively high output resistance and capacitance makes the

TABLE III

SCHOTTKY AND TUNNEL POWER DETECTORS.

parameter	Schottky	tunnel
input bandwidth	up to 4 decades 10 MHz to 20 GHz	1–3 octaves up to 40 GHz
VSVR max.	1.5:1	3.5:1
max. input power (spec.)	-15 dBm	-15 dBm
absolute max. input power	20 dBm or more	20 dBm
output resistance	1–10 kΩ	50–200 Ω
output capacitance	20–200 pF	10–50 pF
gain	300 V/W	1000 V/W
cryogenic temperature	no	yes
electrically fragile	no	yes

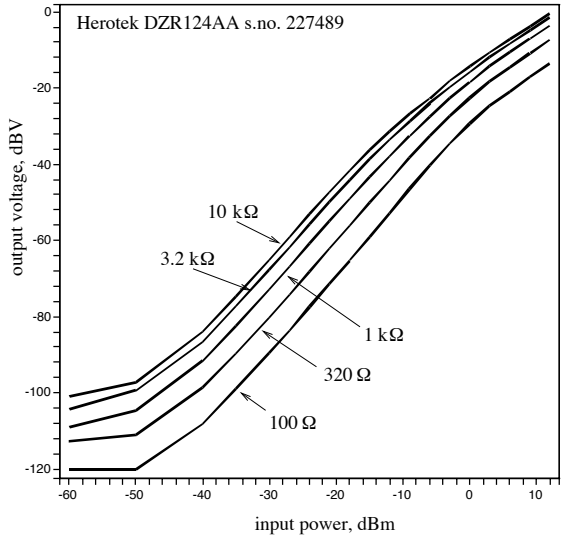

Fig. 3. Measured response of a Schottky detector Herotek DZR124AA.

detector suitable to low-frequency carriers, starting from some 10 MHz (typical). In this condition the current flowing through the diode is small, and the input matching to $R_0 = 50\ \Omega$ is provided by a low value resistor. Thus, the VSWR is close to 1:1 in a wide frequency range. Most of the input power is dissipated in the input resistance, which reduces the risk of damage in case of overload. A strong preference for negative output voltage seems to derive from the lower noise of P type Schottky diodes, as compared to N type ones, in conjunction with practical issues of mechanical layout. The quadratic response [Eq. (13)] derives from the diode differential resistance R_d. At higher input level, R_d becomes too small and the detector response turns smoothly from quadratic to linear, like the response of the common AM demodulators and power rectifiers.

Tunnel detectors are actually *backward* detectors. The backward diode is a tunnel diode in which the negative resistance in the forward-bias region is made negligible by appropriate doping, and used in the reverse-bias region. Most of the work on such detectors dates back to the sixties [3], [4], [5]. Tunnel detectors exhibit fast switching and higher gain than the Schottky counterpart. A low output resistance is necessary, which affects the input impedance. Input impedance matching is therefore poor. If fast response can be sacrificed, the output resistance can be higher than the recommended value, and limited only by noise considerations. At higher output resistance the gain further increases. Tunnel diodes also work in cryogenic environment, provided the package tolerates the mechanical stress.

TABLE IV

MEASURED CONVERSION GAIN.

load resistance, Ω	detector gain, A^{-1} DZR124AA (Schottky)	 DT8012 (tunnel)
1×10^2	35	292
3.2×10^2	98	505
1×10^3	217	652
3.2×10^3	374	724
1×10^4	494	750
conditions: power -50 to -20 dBm		

Figure 3 and Table IV show the conversion gain of two detectors. As expected, the Schottky detector leaves smoothly the quadratic law (true power detection) at some -12 dBm, where it becomes a peak voltage detector. The response of the tunnel detector is quadratic up to a maximum power lower than that of the Schottky diode. This is due to the lower threshold of the tunnel effect. The output voltage shows a maximum at some 0 dBm, then decreases. This is ascribed to the tunnel-diode conduction in the forward region.

FInally, it is worthy mentioning that the double balanced mixer with the inputs in phase can be used as the detector for AM noise measurements [6]. This choice, is not considered here because (1) it is far more cumbersome and complex than a power detector, and (2) the diode technology (Schottky) is the same, hence one can expect similar or lower noise from the detector, which is simpler.

IV. POWER DETECTOR NOISE

Two fundamental types of noise are present in a power detector, shot noise and thermal noise [4, Sec. V]. In addition, detectors show flicker noise. The latter is not explained theoretically, for the detector characterization relies on experimental parameters. Some useful pieces of information are available in [7].

Owing to the shot effect, the average current $\bar{\imath}$ flowing in the diode junction is affected by a fluctuation of power spectral density

$$S_i = 2q\bar{\imath} \qquad \mathrm{A}^2/\mathrm{Hz}, \tag{14}$$

Using the Ohm law $v = Ri$ across the load resistor R, the noise voltage at the detector output is

$$S_v = 2qR\overline{v} \qquad \mathrm{V}^2/\mathrm{Hz}. \tag{15}$$

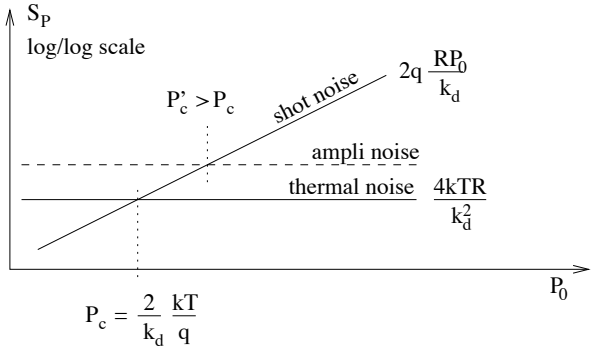

Fig. 4. Power spectral density of the detector noise, referred at the input.

Then, the shot noise is referred to the input-power noise using $v = k_d P$. Thus, at the operating power P_0 it holds that

$$S_P = 2q\frac{RP_0}{k_d} \qquad \text{shot noise, } \mathrm{W}^2/\mathrm{Hz}. \tag{16}$$

The thermal noise across load resistance R has the power spectral density

$$S_v = 4kTR \qquad \mathrm{V}^2/\mathrm{Hz}, \tag{17}$$

which turns into

$$S_P = \frac{4kTR}{k_d^2} \qquad \text{thermal noise, } \mathrm{W}^2/\mathrm{Hz}. \tag{18}$$

referred to the detector input. An additional thermal-noise contribution comes from the dissipative resistance of the diodes. This can be accounted for by increasing the value of R in Equations (17) and (18). It should be remarked that diode differential resistance is not a dissipative phenomenon, for there is no thermal noise associated to it.

Figure 4 shows the equivalent input noise as a function of power. The shot noise is equal to the thermal noise, $(S_P)_{\text{shot}} = (S_P)_{\text{thermal}}$, at the critical power

$$P_c = \frac{2}{k_d}\,\frac{kT}{q}\ . \tag{19}$$

In practice, it turns out that in the quadratic (power-detection) region, shot noise is negligible vs. thermal noise. This can be seen on Figure 3.

Looking at the specifications of commercial power detectors, information about noise is scarce. Some manufacturers give the NEP (Noise Equivalent Power) parameter, i.e., the power at the detector input that produces a video output equal to that of the device noise. In no case is said whether the NEP increases or not in the presence of a strong input signal, which is related to precision. Even worse, no data about flickering is found in the literature or in the data sheets. Only one manufacturer (Herotek) claims the *low flicker* feature of its tunnel diodes, yet without providing any data.

The power detector is always connected to some kind of amplifier, which is noisy. Denoting with $(h_0)_{\text{ampli}}$ and $(h_{-1})_{\text{ampli}}$ the white and flicker noise coefficients of the amplifier, the spectrum density referred at the input is

$$S_P(f) = \frac{(h_0)_{\text{ampli}}}{k_d^2} + \frac{(h_{-1})_{\text{ampli}}}{k_d^d}\,\frac{1}{f}\ . \tag{20}$$

The amplifier noise coefficient $(h_0)_{\text{ampli}}$ is connected to the noise figure by $(h_0)_{\text{ampli}} = (F-1)kT$. Yet we prefer not to use the noise figure because in general the amplifier noise results from voltage noise and current noise, which depends on R. Equation (20) is rewritten in terms of amplitude noise using $\alpha = \frac{1}{2}\frac{\delta P}{P_0}$ [Eq. (6)]. Thus,

$$S_\alpha(f) = \frac{1}{2P_0}\,\frac{qR}{k_d} + \frac{1}{P_0^2}\,\frac{kTR}{k_d^2} + \\ + \frac{1}{4P_0^2}\,\frac{(h_0)_{\text{ampli}}}{k_d^2} + \frac{1}{4P_0^2}\,\frac{(h_{-1})_{\text{ampli}}}{k_d^2}\,\frac{1}{f}\ . \tag{21}$$

After the first term of Eq. (20), the critical power becomes

$$P_c' = \frac{2}{k_d}\,\frac{kT}{q} + \frac{(h_0)_{\text{ampli}}}{2qRk_d}\ . \tag{22}$$

This reinforces the conclusion that in actual conditions the shot noise is negligible.

V. Design of the front-end amplifier

For optimum design, one should account for the detector noise and for the noise of the amplifier, and find the most appropriate amplifier and operating conditions. Yet, the optimum design relies upon the detailed knowledge of the power-detector noise, which is one of our targets (Sec. VI). Thus, we provisionally neglect the excess noise of the power detector. The first design is based on the available data, i.e., thermal noise and the noise of the amplifier. Operational amplifiers or other types of impedance-mismatched amplifiers are often used in practice. As a consequence, a single parameter, i.e., the noise figure or the noise temperature, is not sufficient to describe the amplifier noise. Voltage and current fluctuations must be treated separately, according to the popular Rothe-Dahlke model [8]. The amplifier noise contains white and flicker, thus

$$(S_v)_{\text{ampli}} = h_{0,v} + h_{-1,v}\,\frac{1}{f} \tag{23}$$

$$(S_i)_{\text{ampli}} = h_{0,i} + h_{-1,i}\,\frac{1}{f}\ . \tag{24}$$

The design can be corrected afterwards, accounting for the flicker noise of the detector.

Accounting for shot and thermal noise, and for the noise of the amplifier, the noise spectrum density is

$$S_v = 2qR\overline{v} + 4kTR + (S_v)_{\text{ampli}} + R^2\,(S_i)_{\text{ampli}} \tag{25}$$

at the amplifier input, and

$$S_P = 2q\frac{RP}{k_d} + \frac{4kTR}{k_d^2} + \frac{(S_v)_{\text{ampli}}}{k_d^2} + \frac{R^2\,(S_i)_{\text{ampli}}}{k_d^2} \tag{26}$$

referred to the rf input. The detector gain k_d depends on R, thus the residual S_P can not be arbitrarily reduced by decreasing R. Instead, there is an optimum R at which the system noise is at its minimum.

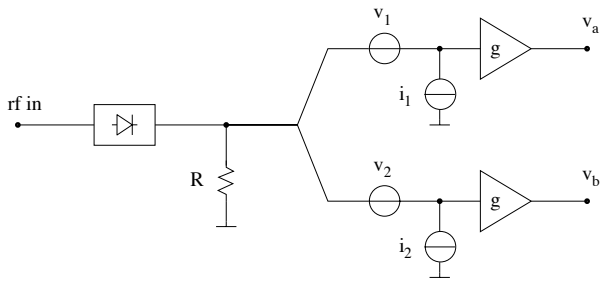

Fig. 5. The load resistor turns the current noise into fully-correlated noise.

The weird case of two paralleled amplifiers

In some cases, it is useful to connect two amplifiers in parallel, at the output of a single detector. This differs from the scheme of Fig. 1 in that correlation rejects only the amplifier noise, provided that the noise of the amplifiers is independent.

For the independence hypothesis to be true, the optimum design of the front-end amplifier changes radically. In fact, the current noise of each amplifier turns into a random voltage fluctuation across the load resistance R (Fig. 5. Focusing only on the amplifier noise, the voltage at the two outputs is

$$v_a = g\,(v_1 + Ri_1 + Ri_2)$$
$$v_b = g\,(v_2 + Ri_1 + Ri_2)$$

The terms gv_1 and gv_2 are independent, for their contribution to the cross spectrum density is reduced by a factor $\frac{1}{\sqrt{2m}}$, where m is the number of averaged spectra. Conversely, a term

$$gR(i_1 + i_2)$$

is present at the two outputs. This term is exactly the same, thus it can not be reduced by correlation and averaging. Consequently, the lowest current noise is the most important parameter, even if this is obtained at expense of a larger voltage noise. Yet, the rejection of larger voltage noise requires large m, for some tradeoff may be necessary. A JFET front-end is often the best choice.

VI. The measurement of the power detector noise

The direct measurement of a detector alone requires that both the noise of the source an the noise of the front-end amplifier are lower than the detector noise, which is unrealistic. Two-diode correlation schemes suffer from the impossibility to measure a single detector. The three-diode scheme of Fig. 6 fixes these problems. It is based on the following ideas.

- The gains are adjusted for the two outputs, $g(P_c - P_a)$ and $g(P_c - P_b)$, to be independent of the AM noise of the source. This is done by observing a null with the lock-in amplifier. The detectors, inherently, are insensitive to residual PM.
- After correlation and averaging, only the signal C is taken. A and B are rejected.

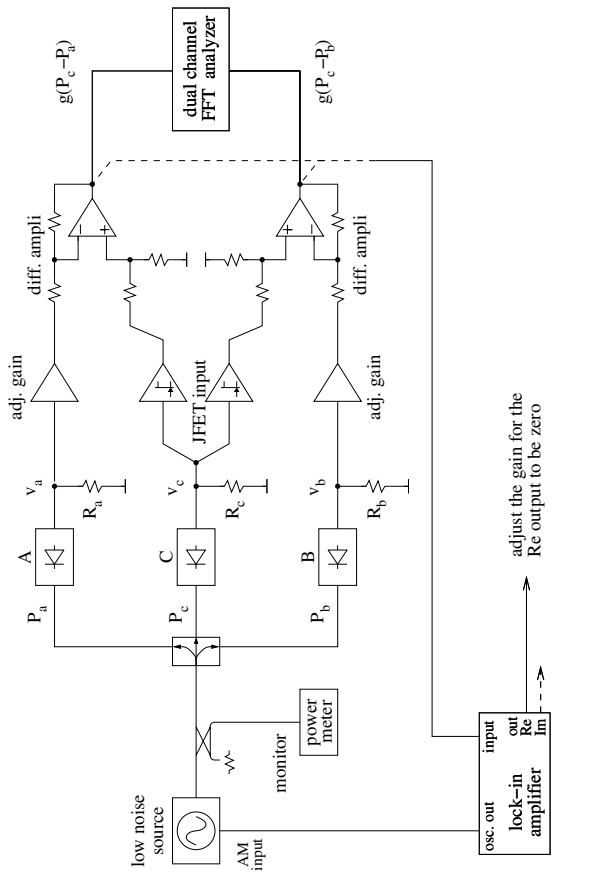

Fig. 6. Improved scheme for the measurement of the power detector noise.

- The diode C has two independent JFET amplifiers, the noise of which is rejected by correlation because the input current noise is negligible. BJT amplifiers, which show lower total noise, are used in channels A and B to speed up the rejection process.

VII. AM noise in optical systems

Equation (1) also describes a quasi-perfect optical, after replacing the voltage $v(t)$ with the electric field. Yet, the preferred physical quantity used to describe the AM noise is the Relative Intensity Noise (RIN), defined as

$$\mathrm{RIN} = S_{\frac{\delta I}{I_0}}(f) \quad , \tag{27}$$

that is, the power spectrum density of the normalized intensity fluctuation

$$\frac{(\delta I)(t)}{I_0} = \frac{I(t) - I_0}{I_0} \quad . \tag{28}$$

The RIN includes both fluctuation of power and the fluctuation of the power cross-section distribution. If the cross-section distribution is constant in time, the optical intensity is proportional to power

$$\frac{\delta I}{I_0} = \frac{\delta P}{P_0} \quad . \tag{29}$$

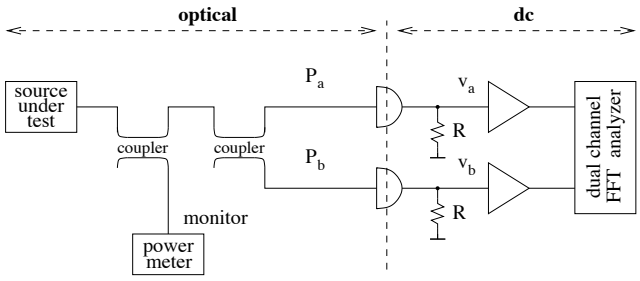

Fig. 7. RIN measurement in optical-fiber systems. In a traditional system, beam splitters are used instead of the couplers.

In optical-fiber system, where the detector collects all the beam power, the term RIN is improperly used for the relative power fluctuation. Reference [9] analyzes on the origin of RIN in semiconductor lasers, while References [10], [11] provide information on some topics of measurement.

In low-noise conditions, $|\delta I/I_0| \ll 1$, and assuming that the cross-section distribution is constant, the power fluctuations are related to the fractional amplitude noise α by

$$\frac{\delta I}{I_0} = \frac{\delta P}{P_0} = 2\alpha \quad , \tag{30}$$

thus

$$\mathrm{RIN}(f) = 4S_\alpha(f) \quad . \tag{31}$$

Generally laser sources show a noise spectrum of the form

$$\mathrm{RIN}(f) = h_0 + h_{-1}f^{-1} + h_{-2}f^{-2} \quad , \tag{32}$$

in which the flicker noise can be hidden by the random walk. Additional fluctuations induced by the environment may be present.

Figure 7 shows the correlation measurement scheme. The output signal of the photodetector is a current proportional to the photon flux. Accordingly, the gain parameter is the detector responsivity ϱ, defined by

$$i = \varrho P \quad , \tag{33}$$

where

$$i = \frac{q\eta P}{h\nu} \tag{34}$$

is the photocurrent, thus

$$\varrho = \frac{q\eta}{h\nu} \quad . \tag{35}$$

Noise is easily analyzed with the methods shown in Section V. Yet in this case the virtual-ground amplifier is often preferred. A book [12] is entirely devoted to the special case of the photodiode amplifier.

VIII. AM NOISE IN MICROWAVE PHOTONIC SYSTEMS

Microwave and rf photonics is being progressively recognized as an emerging domain of technology [13], [14]. It is therefore natural to investigate in noise in these systems.

This section follows the same approach and the same notation of [15]. The power[1] $P_\lambda(t)$ of the optical signal is sinusoidally modulated in intensity at the microwave frequency ν_μ is

$$P_\lambda(t) = \overline{P}_\lambda \left(1 + m\cos 2\pi\nu_\mu t\right) \quad , \tag{36}$$

where m is the modulation index[2]. Eq. (36) is similar to the traditional AM of radio broadcasting, but optical power is modulated instead of RF voltage. In the presence of a distorted (nonlinear) modulation, we take the fundamental microwave frequency ν_0. The detector photocurrent is

$$i(t) = \frac{q\eta}{h\nu_\lambda}\,\overline{P}_\lambda \left(1 + m\cos 2\pi\nu_\mu t\right) \quad , \tag{37}$$

where η the quantum efficiency of the photodetector. The oscillation term $m\cos 2\pi\nu_\mu t$ of Eq. (37) contributes to the microwave signal, the term "1" does not. The microwave power fed into the load resistance R_0 is $\overline{P}_\mu = R_0\overline{i^2}$, hence

$$\overline{P}_\mu = \frac{1}{2}m^2 R_0 \left(\frac{q\eta}{h\nu_\lambda}\,\overline{P}_\lambda\right)^2 \quad . \tag{38}$$

The discrete nature of photons leads to the shot noise of power spectral density $2qiR$ [W/Hz] at the detector output. By virtue of Eq. (37),

$$N_s = 2\frac{q^2\eta}{h\nu_\lambda}\,\overline{P}_\lambda R \qquad \text{(shot noise)} \; . \tag{39}$$

In addition, there is the equivalent input noise of the amplifier loaded by R, whose power spectrum is

$$N_t = FkT \qquad \text{(thermal noise and amplifier noise)} \; , \tag{40}$$

where F is the noise figure of the amplifier, if any, at the output of the photodetector. The white noise $N_s + N_t$ turns into a noise floor

$$S_\alpha = \frac{N_s + N_t}{\overline{P}_\mu} \quad . \tag{41}$$

Using (38), (39) and (40), the floor is

$$S_\alpha = \frac{2}{m^2}\left[2\frac{h\nu_\lambda}{\eta}\,\frac{1}{\overline{P}_\lambda} + \frac{FkT}{R}\left(\frac{h\nu_\lambda}{q\eta}\right)^2\left(\frac{1}{\overline{P}_\lambda}\right)^2\right] \quad . \tag{42}$$

Interestingly, the noise floor is proportional to $(\overline{P}_\lambda)^{-2}$ at low power, and to $(\overline{P}_\lambda)^{-1}$ above the threshold power

$$P_{\lambda,t} = \frac{1}{2}\,\frac{FkT}{R}\,\frac{h\nu_\lambda}{q^2\eta} \tag{43}$$

For example, taking $\nu_\lambda = 193.4$ THz (wavelength $\lambda = 1.55$ μm), $\eta = 0.6$, $F = 1$ (noise-free amplifier), and $m = 1$, we get a threshold power $P_{\lambda,t} = 335$ μW, which sets the noise floor at 5.1×10^{-15} Hz^{-1} (-143 dB/Hz).

Figure 8 shows the scheme of a correlation system for the measurement of the microwave AM noise. It may be necessary to add a microwave amplifier at the output of each

[1] In this section we use the subscript λ for 'light' and μ for 'microwave'.

[2] We use the symbol m for the modulation index, as in the general literature. There is no ambiguity because the number of averages (m) is not used in this section.

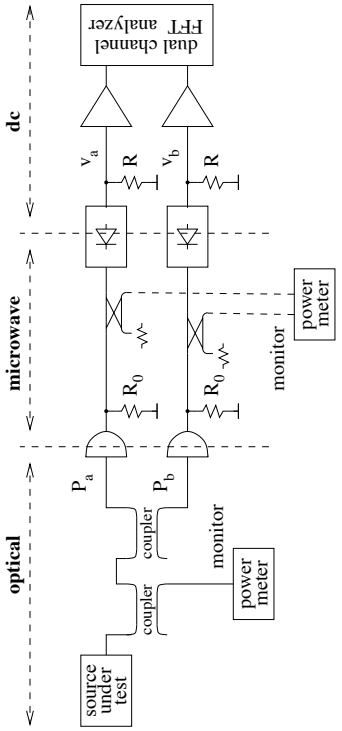

Fig. 8. Measurement of the microwave AM noise of a modulated light beam.

photodetector. Eq. (42) holds for one arm of Fig. 8. As there are two independent arms, the noise power is multiplied by two.

Finally, it is to be pointed out that the results of this section concern only the white noise of the photodetector and of the microwave amplifier at the photodetector output. Experimental method and some data in the close-in microwave flickering of the high-speed photodetectors is available in Reference [16]. The noise of the microwave power detector and of its amplifier is still to be added, according to Section IV.

IX. Calibration

For small variations ΔP around a power P_0, the detector gain is replaced by the differential gain

$$k_d = \frac{dv_d}{dP} \quad . \tag{44}$$

which can be rewritten as

$$k_d = \frac{\Delta v_d}{\frac{\Delta P}{P_0} P_0} \quad . \tag{45}$$

Equations (9)–(10), which are used to get $S_\alpha(f)$ from the spectrum $S_v(f)$ of the output voltage in single-channel measurements, rely upon the knowledge of the calibration factor $k_d P_0$. The separate knowledge of k_d and P_0 is not necessary because only the product $k_d P_0$ enters in Eq. (9)–(10). Therefore we can get $k_d P_0$ from

$$k_d P_0 = \frac{\Delta v_d}{\Delta P / P_0} \quad . \tag{46}$$

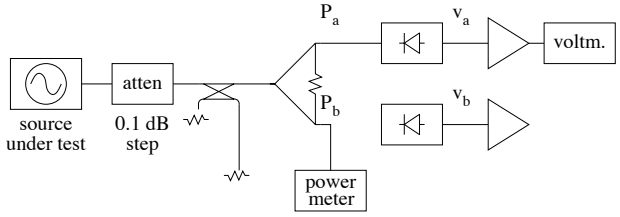

Fig. 9. Simple calibration scheme.

This is a fortunate outcome for the following reasons

- A variable attenuator inserted in series to the oscillator under test sets a static $\delta P/P_0$ that is the same in all the circuit; this is a consequence of linearity. For reference,

step, dB	$\Delta P/P_0$
0.1	2.33×10^{-2}
0.5	0.122
1	0.259

- A power ratio can be measured (or set) more accurately than an absolute power.

Fig. 9 shows a correlation scheme. Symmetry is exploited to measure k_a and k_b in a condition as close as possible to the final measurement of $S_\alpha(f)$. Of course, it holds that $\Delta P_a/P_a = \Delta P_b/P_b$. Other schemes are possible, depending on the available instrumentation. In all cases it is recommended to

- measure the power at the detector input.
- exploit the differential accuracy of the instruments that measure ΔP and ΔV, instead of the absolute accuracy. Use the "relative" function if available, and do not change input range.
- avoid plugging and unplugging connectors during the measurement. Use directional couplers instead.

Alternate calibration method

Another method to calibrate the power detector makes use of two synthesizers in the frequency region of interest, so that the beat note falls in the audio region (Fig. 10). This scheme is inspired to the two-tone method, used to measure the deviation of the detector from the law $v_d = k_d P$ [17], [18].

Using $P = \frac{v^2}{R}$, and denoting the carrier and the reference sideband with $v_0(t) = V_0 \cos(2\pi\nu_0 t)$ and $v_s(t) = V_s \cos(2\pi\nu_s t)$, respectively, the detected signal is

$$v_d(t) = \frac{k_d}{R}\Big\{v_0(t) + v_s(t)\Big\}^2 * h_{lp}(t) \quad . \tag{47}$$

The low-pass function h_{lp} keeps the dc and the beat note at the frequency $\nu_b = \nu_s - \nu_0$, and eliminates the $\nu_s + \nu_0$ terms. Thus,

$$v_d(t) = \frac{k_d}{R}\Big\{\frac{1}{2}V_0^2 + \frac{1}{2}V_s^2 + 2\frac{1}{2}V_0 V_s \cos\big[2\pi(\nu_s - \nu_0)t\big]\Big\} \quad , \tag{48}$$

which is split into the dc term

$$\overline{v}_d = k_d \frac{V_0^2 + V_s^2}{2R} \tag{49}$$

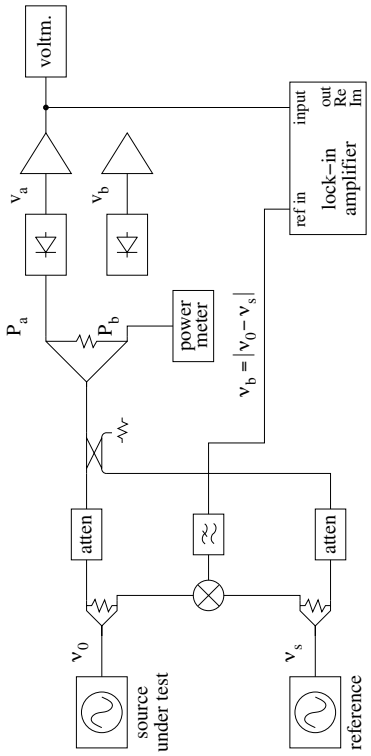

Fig. 10. Alternate calibration schemes.

Wenzel 501-04623E (s/n 3572-0214)
$P_d = 9.5\ \mu$W (-10.2 dBm)
$k_d = 1.31\times10^{5}$ A^{-1} with dc ampli
$m = 2104$ averaged spectra
$\sqrt{2m} = 64.9$ (18.1 dB)
$h_{-1} = 1.5\times10^{-13}$ Hz^{-1} (-128.2 dB)
$\sigma_\alpha = 4.6\times10^{-7}$

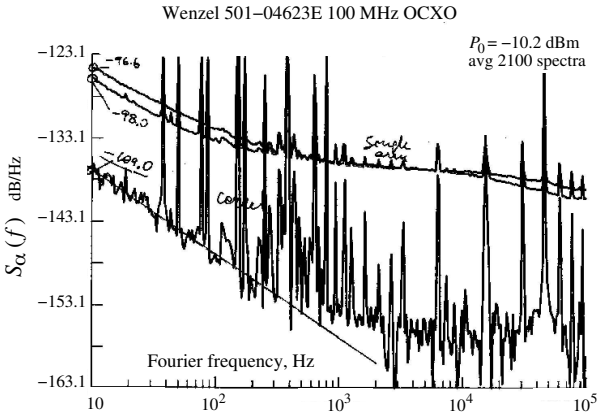

Fig. 11. Example of AM noise measurement. Gain 28.2 dB.

and the beat-note term

$$\tilde{v}_d(t) = 2\,\frac{k_d}{R}\,\frac{V_0 V_s}{2}\cos\left[2\pi(\nu_s - \nu_0)t\right] \quad , \tag{50}$$

hence

$$\left(V_d\right)_{\rm rms} = k_d\sqrt{2P_0P_s} \quad . \tag{51}$$

The dc term [Eq. (49)] makes it possible to measure k_d from the contrast between $\overline{v}_1$, observed with the carrier alone, and $\overline{v}_2$, observed with both signals. Thus,

$$k_d = \frac{\overline{v}_2 - \overline{v}_1}{P_s} \tag{52}$$

Alternatively, the ac term [Eq. (51)] yields

$$k_d = \frac{\left(V_d\right)_{\rm rms}}{\sqrt{2P_0P_s}} \tag{53}$$

The latter is appealing because the assessment of k_d relies only on ac measurements, which are free from offset and thermal drift. On the other hand, the two-tone measurement does not provide the straight measurement of the product k_dP_0.

X. Examples

Figure 11 shows an example of AM noise measurement. The source under test is a 100 MHz quartz oscillator (Wenzel 501-04623E serial no. 3752-0214).

Calibration is done by changing the power $P_0 = -10.2$ dBm by ±0.1 dB. There results $k_a = 1.28\times10^5$ V/W and $k_b = 1.34\times10^5$ V/W, including the 52 dB amplifier (321 V/W and 336 V/W without amplification). The system gain is therefore $4k_ak_bP_aP_b = 641$ V^2 (28.1 dBV^2).

The cross spectrum of Fig. 11 is $S_{ba} = 1.26\times10^{-11}$ V^2 (-109 dBV^2/Hz) at 10 Hz, of the flicker type. Averaging over $m = 2104$ spectra, the single-channel noise is rejected by $\sqrt{2\times2104} = 64.9$ (18.1 dB). The displayed flicker (-109 dB at 10 Hz) exceeds by 6.4 dB the rejected single-channel noise. A correction of a factor 0.77 (-1.1 dB) is therefore necessary. The corrected flicker is $S_{ba} = 9.7\times10^{-12}$ V^2 (-110.1 dBV^2/Hz) extrapolated at 1 Hz. The white noise can not be obtained from Fig. 11 because of the insufficient number of averaged spectra.

As a consequence of the low amplitude noise of the oscillator, it is possible to measure the noise of single channel, which includes detector and amplifier. Accounting for the gain (28.1 dBV^2), the single-channel flicker noise of Fig. 11 at 1 Hz is $S_\alpha(1\,\text{Hz}) = 2.5\times10^{-12}$ Hz^{-1} (-116.1 dB/Hz) for one channel, and $S_\alpha(1\,\text{Hz}) = 3.4\times10^{-12}$ Hz^{-1} (-114.7 dB/Hz) for the other channel.

The AM flickering of the oscillator is $S_\alpha(1\,\text{Hz}) = 1.5\times10^{-13}$ Hz^{-1} (-129.4 dB/Hz), thus $h_{-1} = 1.5\times10^{-13}$. Using the conversion formula of Tab. I for flicker noise, the Allan variance is $\sigma_\alpha^2 = 1.6\times10^{-13}$, which indicates an amplitude stability $\sigma_\alpha = 4.6\times10^{-7}$, independent of the measurement time τ.

Table V shows some examples of AM noise measurement.

All the experiments of Tab. V were done before thinking seriously about the design of the front-end amplifier (Section V), and before measuring the detector gain as a function of the load resistance (Table IV). The available low-noise

TABLE V

AM NOISE OF SOME SOURCES.

source	h_{-1}	σ_α
Anritsu MG3690A synthesizer (10 GHz)	2.5×10^{-11} -106.0 dB	5.9×10^{-6}
Marconi synthesizer (5 GHz)	1.1×10^{-12} -119.6 dB	1.2×10^{-6}
Macom PLX 32-18 $0.1 \rightarrow 9.9$ GHz multiplier	1.0×10^{-12} -120.0 dB	1.2×10^{-6}
Omega DRV9R192-105F 9.2 GHz DRO	8.1×10^{-11} -100.9 dB	1.1×10^{-5}
Narda DBP-0812N733 amplifier (9.9 GHz)	2.9×10^{-11} -105.4 dB	6.3×10^{-6}
HP 8662A no. 1 synthesizer (100 MHz)	6.8×10^{-13} -121.7 dB	9.7×10^{-7}
HP 8662A no. 2 synthesizer (100 MHz)	1.3×10^{-12} -118.8 dB	1.4×10^{-6}
Fluke 6160B synthesizer	1.5×10^{-12} -118.3 dB	1.5×10^{-6}
Racal Dana 9087B synthesizer (100 MHz)	8.4×10^{-12} -110.8 dB	3.4×10^{-6}
Wenzel 500-02789D 100 MHz OCXO	4.7×10^{-12} -113.3 dB	2.6×10^{-6}
Wenzel 501-04623E no. 1 100 MHz OCXO	2.0×10^{-13} -127.1 dB	5.2×10^{-7}
Wenzel 501-04623E no. 2 100 MHz OCXO	1.5×10^{-13} -128.2 dB	4.6×10^{-7}

amplifiers, designed for other purposes, turned out to be a bad choice, far from being optimized for this application. Nonetheless, in all cases the observed cross spectrum is higher than the limit set by the average of two independent single-channel spectra. In addition, the limit set by channel isolation is significantly lower than the observed cross spectrum. These two facts indicate that the measured cross-spectrum is the true AM noise of the source. Thus Table V is an accurate database for a few specific cases. Of course, Table V also provides the order of magnitude for the AM noise of other synthesizers and oscillators employing similar technology. On the other hand, the data of Table V do not provide information on the detector noise.

ACKNOWLEDGEMENTS

I wish to thank Vincent Giordano and Laurent Larger (Femto-St) for support and a number of useful discussions; Franck Lardet-Vieudrin and Cyrus Rocher (Femto-St) for help with electronics. Lute Maleki and John Dick (JPL, Pasadena), gave invaluable suggestions in several occasions.

REFERENCES

[1] E. Rubiola and V. Giordano, "Advanced interferometric phase and amplitude noise measurements," *Rev. Sci. Instrum.*, vol. 73, pp. 2445–2457, June 2002. Also on the web site arxiv.org, document arXiv:physics/0503015v1.

[2] Agilent Technologies, Inc., Paloalto, CA, *Fundamentals of RF and Microwave Power Measurements, Part 1–4*, 2003.

[3] C. A. Burrus, "Backward diodes for low-level millimeter-wave detection," *IEEE Trans. Microw. Theory Tech.*, vol. 11, pp. 357–362, Sept. 1963.

[4] W. F. Gabriel, "Tunnel-diode low-level detection," *IEEE Trans. Microw. Theory Tech.*, vol. 15, pp. 538–553, Oct. 1967.

[5] R. N. Hall, "Tunnel diodes," *IRE Trans. Electron Dev.*, vol. (?), pp. 1–9, Sept. 1960.

[6] L. M. Nelson, C. Nelson, and F. L. Walls, "Relationship of AM to PM noise in selected RF oscillators," *IEEE Trans. Ultras. Ferroelec. and Freq. Contr.*, vol. 41, pp. 680–684, May 1994.

[7] S. T. Eng, "Low-noise properties of microwave backward diodes," *IRE Trans. Microw. Theory Tech.*, vol. 9, pp. 419–425, Sept. 1961.

[8] H. Rothe and W. Dahlke, "Theory of noisy fourpoles," *Proc. IRE*, vol. 44, pp. 811–818, June 1956.

[9] C. B. Su, J. Schiafer, and R. B. Lauer, "Explanation of low-frequency relative intensity noise in semiconductor lasers," *Appl. Phys. Lett.*, vol. 57, pp. 849–851, Aug. 27 1990.

[10] I. Joindot, "Measurement of relative intensity noise (RIN) in semiconductor lasers," *J. Phys. III France*, vol. 2, pp. 1591–1603, Sept. 1992.

[11] G. E. Obarski and J. D. Splett, "Transfer standard for the spectral density of relative intensity noise of optical fiber sources near 1550 nm," *J. Opt. Soc. Am. B - Opt. Phys.*, vol. 18, pp. 750–761, June 2000.

[12] J. G. Graeme, *Photodiode Amplifiers*. Boston (MA): McGraw Hill, 1996.

[13] W. S. C. Chang, ed., *RF Photonic Technology in Optical Fiber Links*. Cambridge, UK: Cambridge, 2002.

[14] A. Seeds, P. Juodawlkis, J. Marti, and T. Nagatsuma, eds., *IEEE Transactions on Microwave Theory and Techniques, Special Issue on Microwave Photonics*. IEEE, Feb. 2006.

[15] E. Rubiola, E. Salik, S. Huang, and L. Maleki, "Photonic delay technique for phase noise measurement of microwave oscillators," *J. Opt. Soc. Am. B - Opt. Phys.*, vol. 22, pp. 987–997, May 2005.

[16] E. Rubiola, E. Salik, N. Yu, and L. Maleki, "Flicker noise in high-speed p-i-n photodiodes," *IEEE Trans. Microw. Theory Tech.*, vol. 54, pp. 816–820, Feb. 2006. Preprint available on arxiv.org, document arXiv:physics/0503022v1, March 2005.

[17] V. S. Reinhardt, Y. Shih, P. A. Toth, S. C. Reynolds, and A. L. Berman, "Methods for measuring the power linearity of microwave detectors for radiometric applications," *IEEE Trans. Microw. Theory Tech.*, vol. 43, pp. 715–720, Apr. 1995.

[18] D. K. Walker, K. J. Coakley, and J. D. Splett, "Nonlinear modeling of tunnel diode detectors," in *Proc. 2004 IEEE International Geoscience and Remote Sensing Symposium (IGARSS '04)*, vol. 6, pp. 3969–3972, 2004.